J. Fluid Mech. (1999), *vol.* 397, *pp.* 317–330. Printed in the United Kingdom

A spatial analogue of transient growth in plane Couette flow

By JACQUES VANNESTE

Department of Mathematics and Statistics, University of Edinburgh,
James Clerk Maxwell Building, King's Buildings, Mayfield Road, Edinburgh EH9 3JZ, UK

(Received 26 January 1997 and in revised form 21 June 1999)

The linear response of an inviscid two-dimensional Couette flow disturbed by a time-periodic forcing is studied under the assumption that the forcing is distributed along a straight line. When the forcing is tilted against the shear, the disturbance streamfunction and energy are shown to be locally amplified downstream of the source before decaying at large distance. This spatially localized amplification is interpreted as an analogue of the transient growth phenomenon studied in the context of unforced intial-value problems. The self-consistency of the linear approximation and the instability of the disturbance are also examined.

1. Introduction

In the last fifteen years or so, the linear evolution of disturbances in spectrally stable shear flows has attracted renewed attention, following the re-examination of the classical work of Lord Kelvin (Thomson 1887) and Orr (1907) by several researchers. The main reason for this attention is the possibility of transient growth of the disturbance amplitude as measured by some norm (generally the disturbance energy). This growth takes place only for certain classes of initial excitation (Shepherd 1985); it essentially depends on the definition of the norm; and it is inevitably followed by a decay in the long-time limit (which is sometimes referred to as Landau damping). Nevertheless, the transient growth mechanism is thought to be relevant to a variety of fluid dynamical applications (see e.g. the recent review by Farrell & Ioannou 1996), including error dynamics in weather forecasting (e.g. Farrell 1990), linear dynamics of stochastically forced shear flows (e.g. Farrell & Ioannou 1993), and transition to turbulence (e.g. Trefethen *et al.* 1993; Henningson, Gustavsson & Breuer 1994).

Like most aspects of stability theory, transient growth is generally studied in the context of initial-value problems. Here, we shall be concerned with an analogue of transient growth that arises in a somewhat different context, namely shear flows subject to spatially localized time-periodic forcing. For such flows, a canonical problem is the so-called signalling problem (e.g. Huerre & Monkewitz 1985, 1990; see also Briggs 1964): assuming absolute stability but (possibly) convective instability, one studies the spatial development of the disturbance at a large distance from the forcing. In the same way that standard spectral stability neglects transient growth by focusing on the long-time behaviour of the disturbance, the signalling problem, by focusing on the long-distance behaviour, does not take into account the possibility of spatially localized growth of the disturbance energy. The aim of this note is to point out that such a growth is possible in flows which are both absolutely and convectively stable.

To this end, we consider a two-dimensional inviscid Couette flow disturbed by a time-periodic vorticity source which is distributed along a straight line. The resulting vorticity and streamfunction are derived in § 2 using Laplace transform techniques. The vorticity, which is generated at the source, is advected downstream by the basic flow, while constant-vorticity lines initially parallel to the source are tilted by the shear. As a result the spatial scale of the vorticity field decreases at large distances from the source, leading to a decay of the disturbance streamfunction and energy through phase mixing. However, when the vorticity source is tilted *against* the shear, the decrease in the scale of the vorticity is preceded by an increase which extends over a finite distance. This causes a growth of the streamfunction and of the energy localized downstream of the source.

The analogy between the spatial development of the disturbance just described and the well-known time evolution of sheared disturbances which are associated with transient growth is obvious. The spatial and temporal problems are nevertheless not formally equivalent; and, for the spatial problem studied here, the disturbance streamfunction is expressed as an integral which cannot be evaluated analytically. In § 3 we present results of three numerical integrations that illustrate the different behaviour of the disturbance streamfunction and energy obtained for different vorticity sources. These results, which are derived for a channel geometry, highlight the effect of the boundaries in the spatial distribution of the energy. Additional aspects of the spatial development of the disturbance are examined. The long-distance behaviour is analysed in § 4 where we derive an asymptotic expression showing that the decay of the streamfunction is proportional to x^{-2}, where x is the distance from the source. This decay is analogous to the t^{-2} decay found for transient sheared disturbances (e.g. Brown & Stewartson 1980), and it can be regarded as the fluid dynamical equivalent of the spatial Landau damping studied in plasma physics (e.g. Ichimaru 1973). Two other properties that have been previously investigated in the context of transient sheared disturbances are discussed in § 5: following Tung (1983), we show that the linearization of the disturbance dynamics is self-consistent, although the vorticity gradient increases without bound with the distance from the source; and, following Haynes (1987), we study the stability of the disturbance to infinitesimal perturbations. Assuming a low-frequency forcing, an instability is shown to occur, but because of the stabilizing effect of the boundaries, only at sufficiently large distance downstream of the source.

2. Analytical results

2.1. *Vorticity*

We consider the Couette flow of an inviscid two-dimensional incompressible fluid. Using x and y as streamwise and cross-stream coordinates, the basic-flow velocity field is written

$$(U, V) = (\lambda y + \mu, 0),$$

where λ and μ are positive constants, and the fluid domain is defined by $(x, y) \in (-\infty, \infty) \times [0, L]$, corresponding to an infinite channel of width L. The evolution of disturbances in this shear flow is governed by the vorticity equation

$$[\partial_t + U(y)\partial_x]\,\omega + \partial(\psi, \omega) = f, \tag{2.1}$$

where ψ is the disturbance streamfunction, $\omega = \nabla^2\psi$ the disturbance vorticity, $\partial(\cdot, \cdot)$ the Jacobian operator, and $f = f(x, y, t)$ is a vorticity source (or sink) term. Physically,

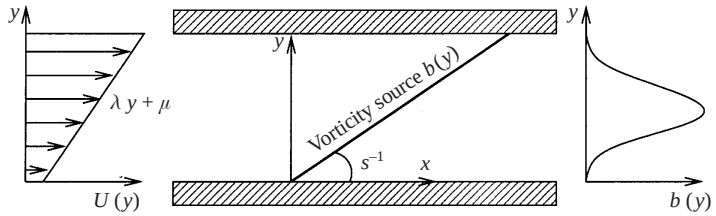

FIGURE 1. Schematic of the system studied: a two-dimensional flow $U(y) = \lambda y + \mu$ in a channel is disturbed by an oscillatory vorticity source distributed along a straight line with slope s^{-1}. The distribution of the vorticity source along this straight line is given by $b(y)$.

a vorticity source appears when a rotational surface stress is applied to the fluid (f is then the curl of the stress), or, for rotating fluids, in the presence of a mass source (which must then scale like the Rossby number for the flow to remain quasi-two-dimensional). Here, we shall be concerned with a source term which is periodic in time, localized on a straight line in space, and has a weak amplitude, so f takes the form

$$f(x, y, t) = \epsilon b(y)\delta(x - sy)\cos(\Omega t),$$

where $\epsilon \ll 1$ is an amplitude parameter and Ω a frequency. The function $b(y)$ determines the distribution of the vorticity source along the straight line which is defined by $x - sy = 0$ and thus has a slope s^{-1}. The configuration of the system is sketched in figure 1.

It is convenient to non-dimensionalize (2.1) using L and Ω^{-1} as reference length and time, and to scale ω and ψ by ϵ. Neglecting the nonlinear term $\epsilon\partial(\psi, \omega)$, we obtain the linear vorticity equation in non-dimensional form

$$[\partial_t + U(y)\partial_x]\,\omega = b(y)\delta(x - sy)\cos t\, e^{\sigma t}. \tag{2.2}$$

The real exponential, with $0 < \sigma \ll 1$, is introduced to impose causality; σ will be taken equal to zero at the end of the calculation. Neglecting the transient, the vorticity is written

$$\omega(x, y, t) = \mathrm{Re}\left[\hat{\omega}(x, y)\, e^{(i+\sigma)t}\right].$$

Let $\hat{\omega}_k(y)$ be the Fourier transform of $\hat{\omega}(x, y)$ defined by the relations

$$\hat{\omega}_k(y) = \frac{1}{\sqrt{2\pi}}\int_{-\infty}^{\infty}\hat{\omega}(x, y)\, e^{-ikx}\,dx \quad \text{and} \quad \hat{\omega}(x, y) = \frac{1}{\sqrt{2\pi}}\int_{-\infty}^{\infty}\hat{\omega}_k(y)\, e^{ikx}\,dk. \tag{2.3}$$

After introducing (2.3) into (2.2), $\hat{\omega}_k(y)$ is found to satisfy

$$\hat{\omega}_k(y) = \frac{-ib(y)\, e^{-iksy}}{\sqrt{2\pi}\,[U(y)\,k + 1 - i\sigma]}. \tag{2.4}$$

Inverting the Fourier transform according to (2.3) leads to

$$\hat{\omega}(x, y) = \frac{-ib(y)}{2\pi}\int_{-\infty}^{\infty}\frac{e^{ik(x-sy)}}{U(y)\,k + 1 - i\sigma}\,dk.$$

In the complex plane for k, the integration contour can be closed in the upper half-plane for $x - sy > 0$ and in the lower half-plane for $x - sy < 0$. Since $U(y)$ and σ are

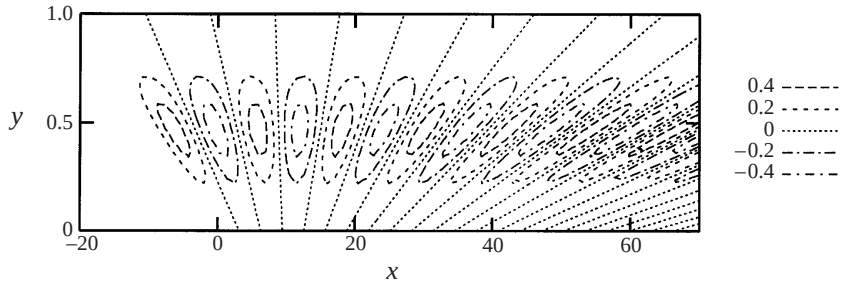

FIGURE 2. Vorticity field defined by (2.5) with $t = \pi/2$ and $s = -20$, corresponding to a vorticity source distributed along the straight line $x + 20y = 0$ (i.e. going from the origin to the upper left corner of the frame).

both positive, the residue theorem then gives

$$\hat{\omega}(x, y) = \frac{b(y)}{U(y)} \, \mathrm{e}^{-\mathrm{i}\frac{x-sy}{U(y)}} H(x - sy),$$

where $H(\cdot)$ is the Heaviside function and σ is set equal to zero. The vorticity is finally given by

$$\omega(x, y, t) = \frac{b(y)}{U(y)} \cos\left[\frac{x - sy}{U(y)} - t\right] H(x - sy). \tag{2.5}$$

Note that the same result can be derived by transforming the coordinates (x, y, t) in (2.2) into the convected coordinate system $(x - U(y)t, y, t)$.

As an illustration, we show in figure 2 the vorticity distribution (2.5) for the following parameter values: $\lambda = \mu = 1$, $s = -20$. The function $b(y)$ is taken as a Gaussian centred on the middle of the channel and with a half-width of 0.25 ((3.1) below, with $\Delta = 0.25$). For convenience we have chosen to draw the figure for $t = \pi/2$, when the vorticity is continuous across the source, but it is fairly simple to visualize the evolution of the vorticity which is continuously advected and sheared by the basic flow. The constant-vorticity lines get tilted as the distance from the source increases, leading to a decrease of the spatial scale, as they do when time increases for transient sheared disturbances. The overall picture of the vorticity distribution defined by (2.5) is nevertheless somewhat different from that obtained for transient sheared disturbances; if one were to mimic the 'Venitian-blind' comparison often used for transient disturbances, one could speak here of a 'fan' structure for the vorticity. The consequences of this structure for the streamfunction are now analysed.

2.2. *Streamfunction*

The streamfunction is obtained from the Poisson equation $\nabla^2\psi = \omega$ which can be solved using a Green's function. Employing for ψ a notation similar to that employed for ω, we find

$$\hat{\psi}(x, y) = \frac{-\mathrm{i}}{2\pi} \int_0^1 b(y') \, \mathrm{d}y' \int_{-\infty}^{\infty} \frac{G(y, y', k) \, \mathrm{e}^{\mathrm{i}k(x-sy')}}{U(y') \, k + 1 - \mathrm{i}\sigma} \, \mathrm{d}k, \tag{2.6}$$

where, for the geometry considered, the Green's function is

$$G(y, y', k) = \frac{-\sinh(ky_<)\sinh[k(1 - y_>)]}{k \sinh k}, \qquad \text{with } y_< := \min(y, y') \text{ and } y_> := \max(y, y'). \tag{2.7}$$

The integral in k can be evaluated using the residue theorem. Taking into account the poles of the Green's function at $k = \pm i\pi, \pm 2i\pi, \ldots$ leads to

$$\hat{\psi}(x, y) = \int_0^1 b(y') J(x - sy', y, y')\, \mathrm{d}y', \tag{2.8}$$

where

$$J(x, y, y') = \begin{cases} \displaystyle\sum_{n=1}^{\infty} \frac{(-1)^n}{n\pi} \frac{K(y, y', n)\, \mathrm{e}^{n\pi x}}{n\pi U(y') + \mathrm{i}}, & x < 0 \\ \displaystyle\sum_{n=1}^{\infty} \frac{(-1)^{n+1}}{n\pi} \frac{K(y, y', n)\, \mathrm{e}^{-n\pi x}}{n\pi U(y') - \mathrm{i}} + \frac{G\big(y, y', 1/U(y')\big)\, \mathrm{e}^{-\mathrm{i}\frac{x}{U(y')}}}{U(y')}, & x > 0 \end{cases} \tag{2.9}$$

and $K(y, y', n) := \sin(n\pi y_<) \sin[n\pi(1 - y_>)]$. Two remarks should be made. First, the series present in the definition of $J(x, y, y')$ converge for any value of x. Since these series decay exponentially with $|x|$, it is clear from (2.8) that they contribute significantly to the streamfunction only in the vicinity of the vorticity source, i.e. for x in the vicinity of $[0, s]$ when $s > 0$ ($[s, 0]$ when $s < 0$). Second, J is continuous at $x = 0$. This property, which may not be directly obvious from (2.9), results from the rapid decay of the integrand of (2.6) when $|k| \to \infty$ and from the consequent vanishing of the sum of its residues. The continuity of J is in fact necessary to ensure that $\hat{\psi}(x, y)$ is continuous across the vorticity source when $s = 0$.

A numerical integration is in general required to evaluate the streamfunction from (2.8)–(2.9), and results of such an integration are presented in the next section. We can however discuss the essential properties of the streamfunction by examining its analytical expression, which, away from the source, can be approximated by

$$\hat{\psi}(x, y) \approx \begin{cases} 0, & x < \min[0, s] \\ \mathrm{e}^{\mathrm{i}\phi} \displaystyle\int_0^1 \frac{b(y') G\big(y,\, y',\, 1/U(y')\big)\, \mathrm{e}^{-\mathrm{i}\frac{\xi}{U(y')}}}{U(y')}\, \mathrm{d}y', & x > \max[0, s], \end{cases} \tag{2.10}$$

where we have written

$$\frac{x - sy}{U(y)} = \frac{\xi}{U(y)} - \phi, \quad \text{with} \quad \xi = x - x_\mathrm{m} := x + s\mu/\lambda \quad \text{and} \quad \phi = s/\lambda.$$

The Riemann–Lebesgue lemma indicates that the integral tends to zero for large ξ. Far downstream of the source, the streamfunction $\hat{\psi}$ thus experiences an inviscid damping due to the shear. This damping is analogous to the spatial Landau damping studied in plasmas (e.g. Ichimaru 1973), and it is the spatial counterpart of the long-time decay associated with free disturbances in shear flows (e.g. Brown & Stewartson 1980). Since the Green's function is only twice differentiable, one can anticipate that $\hat{\psi}$ decays like x^{-2}; this is confirmed in § 4, where the asymptotic form of $\hat{\psi}$ is derived.

If $s > 0$, i.e. if the source is tilted with the shear, x_m is negative and thus ξ is positive everywhere downstream of the source; the phase mixing is therefore minimized at the source, so that $\hat{\psi}$ attains its maximum in its vicinity, for $x \approx sy$, and decreases monotically downstream. If $s < 0$ however, i.e. if the source is tilted against the shear, x_m is positive and the situation is very different. Indeed, in this case, ξ and thus the phase mixing vanish for $x = x_\mathrm{m}$, leading to a maximum of the streamfunction in the vicinity of x_m rather than near the source. The streamfunction is thus locally amplified downstream of the source before decaying at long distance. This local amplification

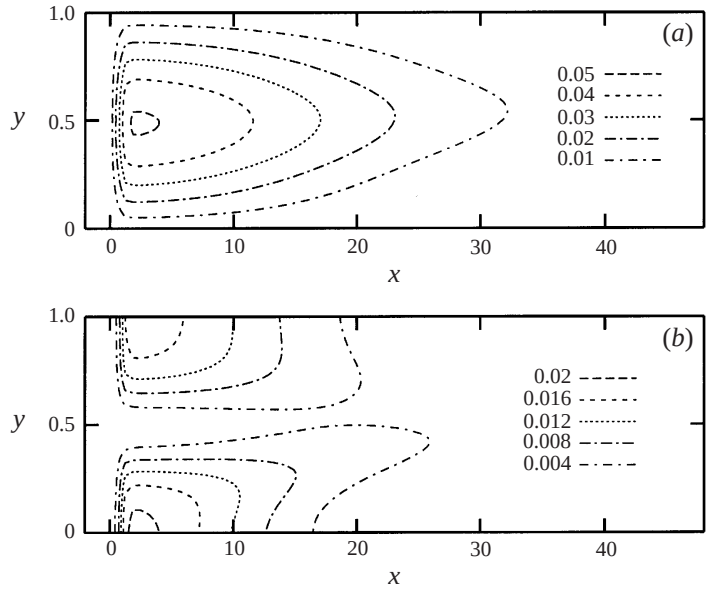

FIGURE 3. Amplitude of the streamfunction $|\psi|$ (a) and energy density E (b) for a vorticity source distributed along the line $x = 0$.

is the spatial analogue of the transient growth phenomenon. (The effect is of course most spectacular when the vorticity source is strongly tilted against the shear, e.g. when $s \ll -1$, since the maximum is then located at great distance from the source.)

Generally the transient growth phenomenon is discussed in terms of disturbance energy rather than streamfunction. The same can be done here by considering the time-averaged energy density

$$E(x, y) := \frac{1}{4\pi} \int_0^{2\pi} |\nabla \psi(x, y, t)|^2 \, \mathrm{d}t = \tfrac{1}{4} |\nabla \hat{\psi}(x, y)|^2. \tag{2.11}$$

The arguments employed for the streamfunction carry over for this energy density, which can also be shown to decrease like x^{-2} at long distance and be locally amplified downstream of the source when $s < 0$.

3. Numerical results

In this section, we confirm the qualitative insight provided by the analysis of the analytical expression (2.10) by evaluating the complete expressions (2.8)–(2.9) numerically for three examples. We compute both the streamfunction $\hat{\psi}$ and the energy density E. The numerical integration of (2.8) is straightforward, although it may be noted that the convergence of the series in (2.9) is quite slow when $x = 0$. For each example, we have used for the source a Gaussian distribution centred in the middle of the channel, i.e.

$$b(y) = \exp\left[-\left(\frac{y - 1/2}{\Delta} \right)^2 \right], \tag{3.1}$$

where Δ is the half-width, and we have taken $\lambda = \mu = 1$.

The first example corresponds to $\Delta = 0.25$ and $s = 0$, i.e. to a vorticity source

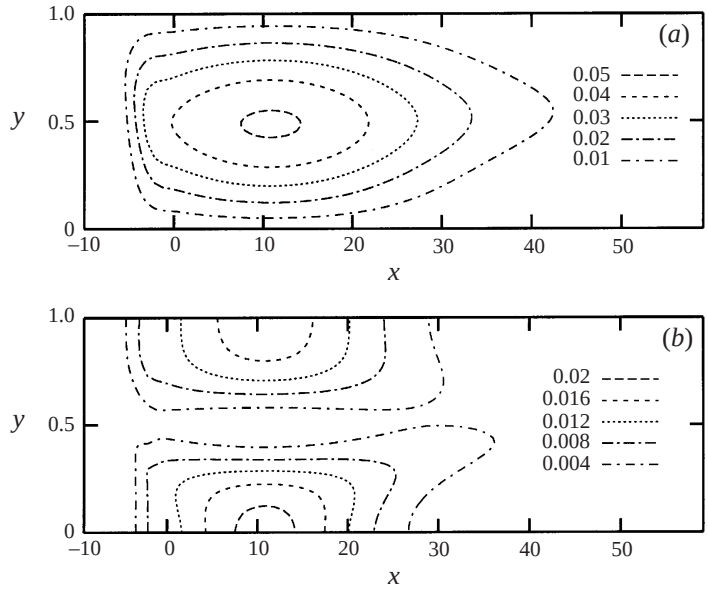

FIGURE 4. Amplitude of the streamfunction $|\psi|$ (*a*) and energy density E (*b*) for a vorticity source distributed along the straight line $x + 10y = 0$ (i.e. going from the origin to the upper left corner of the frame).

perpendicular to the shear (at $x = 0$), in which case we expect the streamfunction ψ and the energy density E to be maximized near the source and decay downstream. This clearly appears in figure 3 which shows $|\psi(x, y)| = |\hat{\psi}(x, y)|$ and $E(x, y)$. Note that the two fields are not symmetric with respect to $y = \frac{1}{2}$ because of the presence of $U(y)$ in (2.9). Note also that E is maximum at the boundaries and weak in the wake of the vorticity source; this is because $\partial_y \hat{\psi}$, which contributes dominantly to the energy density, is small in the centre of the channel.

The local amplification downstream of the source which is the focus of this paper requires $s < 0$. It is illustrated in figure 4 obtained for $s = -10$ and $\Delta = 0.25$. The maxima of $|\psi|$ and E are observed, as expected, for $x \approx x_m = 10$. Interestingly, there is no sign of an enhancement of $|\psi|$ or E near the source, but the two fields attain significant values upstream of the source for $y < 0.5$, in contrast to the $s = 0$ case.

A somewhat different picture is obtained when the vorticity source is narrowly distributed around $y = \frac{1}{2}$. Figure 5 corresponds to $\Delta = 0.05$ in (3.1), and to $s = -20$. In this case, both $|\psi|$ and E start increasing abruptly when $x = -10$ (the position of the centre of the vorticity source) regardless of y. Note also that the maxima of E are now located inside the channel rather than on the boundaries, although E is still weak in the wake of the source.

4. Asymptotic results

It is clear from (2.8)–(2.10) that an asymptotic formula for the streamfunction $\hat{\psi}$ can be derived for $|\xi| \gg 1$. Such a formula is not only useful to quantify the damping of the streamfunction and energy in the limit $x \gg 1$: in the case of a source strongly tilted against the shear (i.e. $s \ll -1$) the assumption $|\xi| \gg 1$ may also be valid between the source and x_m, and thus the asymptotic formula may describe part of the amplification of the streamfunction and of the energy.

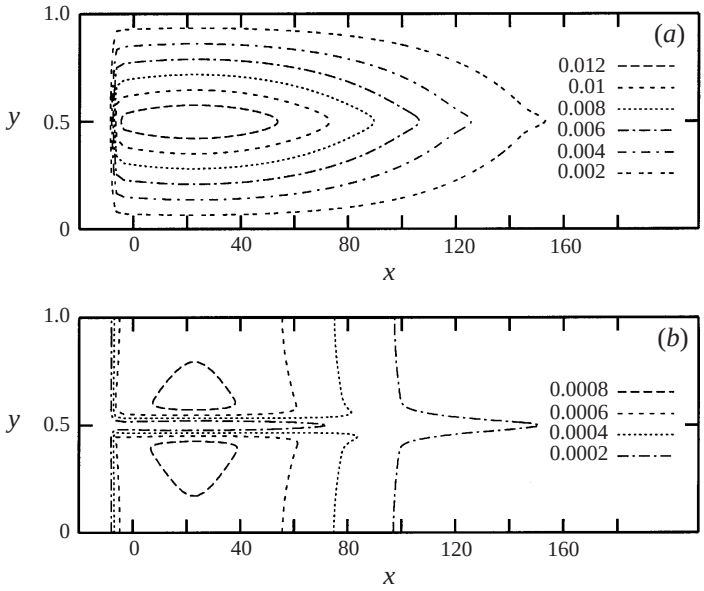

FIGURE 5. Same as figure 4, but with a narrow distribution of vorticity ($\Delta = 0.05$ in (3.1), as opposed to 0.25) on the straight line $x + 20y = 0$.

The asymptotic formula is derived by introducing the variable $\eta' := 1/U(y')$ into (2.10) to obtain

$$\hat{\psi}(x, y) = \frac{\mathrm{e}^{\mathrm{i}\phi}}{\lambda} \int_{\eta_1}^{\eta_0} \frac{b[y'(\eta')]\, G(y, y'(\eta'), \eta')\, \mathrm{e}^{-\mathrm{i}\xi\eta'}}{\eta'}\, \mathrm{d}\eta',$$

where $\eta_1 := 1/U(1)$ and $\eta_0 := 1/U(0)$, and by integrating twice by parts. The final result takes the form

$$\hat{\psi}(x, y) = \frac{\mathrm{e}^{\mathrm{i}\phi}}{\lambda^2\xi^2} \left\{ \frac{b(0) \sinh\left[\eta_0(1-y)\right] \mathrm{e}^{-\mathrm{i}\eta_0\xi}}{\eta_0^3 \sinh\eta_0} + \frac{b(1) \sinh\left(\eta_1 y\right) \mathrm{e}^{-\mathrm{i}\eta_1\xi}}{\eta_1^3 \sinh\eta_1} - \frac{b(y)\, \mathrm{e}^{-\mathrm{i}\eta\xi}}{\eta^3} \right\} + O\left(\frac{1}{\lambda^3\xi^3}\right), \quad (4.1)$$

where $\eta := 1/U(y)$. This confirms that the streamfunction decreases like ξ^{-2} for $\xi \gg 1$, as mentioned in § 2. If the source term vanishes on the channel boundaries, i.e. if $b(0) = b(1) = 0$, the streamfunction can be written as

$$\psi(x, y, t) = -\frac{b(y)[U(y)]^3}{\lambda^2(x - x_\mathrm{m})^2} \cos\left[\frac{x - sy}{U(y)} - t\right] + O\left(\frac{1}{\lambda^3(x - x_\mathrm{m})^3}\right), \quad (4.2)$$

using the definitions of ξ and ϕ. Comparing with the expression (2.5) for the vorticity indicates that the streamfunction and the vorticity oscillate with the same wavenumber in the x-direction. It is not so when $b(0) \neq 0$ or $b(1) \neq 0$ since the streamfunction then has additional oscillations with wavenumbers η_0 or η_1 at all positions in y.

To test the validity of the asymptotic formula for the streamfunction (4.1), we compare it to a numerical evaluation of the exact expression (2.8)–(2.9) in a particular case. The parameters are chosen as $\lambda = \mu = 1$ and $s = -40$, yielding $x_\mathrm{m} = 40$; the distribution of the vorticity source is taken as $b(y) = 1$, so that the contribution of

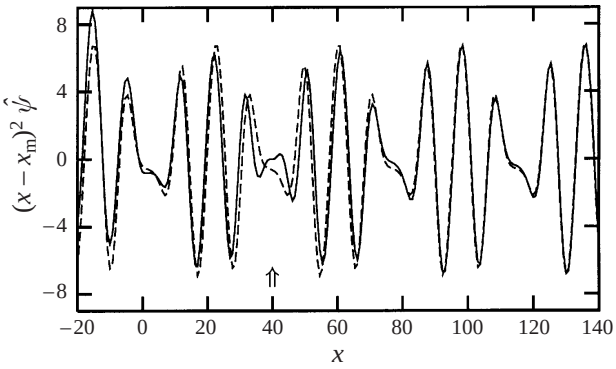

FIGURE 6. Comparison between the exact streamfunction (solid line) and the asymptotic expression (4.1) valid for large $|x - x_m|$ (dashed line), for $y = \frac{1}{2}$ with $\lambda = \mu = b(y) = 1$ and $s = -40$. The streamfunction is scaled by the factor $(x - x_m)^{-2}$ which governs the leading-order behaviour of the asymptotic expression, and x_m is indicated by an arrow.

the boundary terms in (4.1) is significant. Figure 6 shows the comparison at $y = \frac{1}{2}$. The asymptotic solution is seen to approximate the exact one correctly both for $\xi = x - x_m \gg 1$ and $\xi \ll -1$. Of course, when $\xi \ll -1$, the asymptotic expression becomes invalid in the vicinity of the vorticity source, which is located between $x = -40$ and $x = 0$, for the series in (2.9) are not negligible there.

5. Nonlinearity and instability

5.1. *Self-consistency of the linearization*

The disturbances studied here, like transient sheared disturbances, have a very fine structure; indeed, (2.5) indicates that the vorticity gradient increases linearly with x (instead of t for the transient disturbances). This observation raises the question of self-consistency of the linearization of the disturbance equation (2.2) – that is, the question of the possible secular role of the nonlinear terms which may invalidate the linearization. For transient disturbances, this question has been addressed by Tung (1983) who concluded that the linearization remains self-consistent, essentially because the growth of the vorticity gradient is compensated by the decrease of the streamfunction. Not surprisingly the same argument holds here. Since the vorticity source has an amplitude $\epsilon \ll 1$, it is easy to show from the asymptotic expressions (4.1)–(4.2) that the nonlinear term is small even for large x, where the vorticity gradient is large; indeed, the following estimates hold for the nonlinear term:

$$\epsilon\partial(\psi,\omega) = \begin{cases} O\left(\dfrac{\epsilon}{(x-x_m)^2}\right) & \text{if } b(0) = b(1) = 0, \\ O\left(\dfrac{\epsilon}{x-x_m}\right) & \text{if } b(0) \neq 0 \text{ or } b(1) \neq 0. \end{cases} \tag{5.1}$$

These estimates are valid for the disturbance self-interaction, but similar ones can be derived for the interaction between several disturbances provided that they are similar, in the sense that the orders of magnitude of their spatial scales are the same at each location in the flow. By contrast, the nonlinear interaction between disturbances with very different scales can be significant. A consequence of this is the instability of the disturbance (2.5) which we now discuss.

5.2. *Instability*

The solution (2.5) is characterized by a cross-stream vorticity gradient which changes sign (see figure 2); this often indicates a possible barotropic instability since Rayleigh's necessary condition for instability is then satisfied locally. Noting a similar feature for transient sheared disturbances, Haynes (1987) studied their stability in the context of an unbounded flow on a β-plane. He showed analytically that, in the long-wave limit, these disturbances are unstable, and confirmed his findings using numerical simulations. Here we adapt his analytical study to the time-periodic disturbance (2.5). We only sketch the analysis and refer the reader to Haynes (1987) for more details.

The spatial analogue of the long-wave limit employed by Haynes (1987) for transient disturbances is the low-frequency limit. To consider this limit, we need to reintroduce the frequency Ω of the vorticity forcing which has been used as an inverse time scale in the non-dimensionalization of § 2. The time scale is fixed by the amplitude of the shear, so that $\lambda = 1$, or more generally $\lambda = O(1)$. We study the stability of a disturbance with a weak amplitude $\epsilon \ll 1$ at large distance from the source, i.e. with x such that $\xi = x - x_{\mathrm{m}} \gg 1$, so that the asymptotic form of the streamfunction (4.2) is valid. The vorticity and streamfunction of the disturbance whose stability is studied take the form

$$\omega(x, y, t) = \frac{b(y)}{U(y)} \cos\left[\Omega\left(\frac{\xi}{U(y)} - \phi - t\right)\right] + O(\epsilon^3), \tag{5.2}$$

$$\psi(x, y, t) = -\frac{b(y)\,[U(y)]^3}{\lambda^2 \Omega^2 \xi^2} \cos\left[\Omega\left(\frac{\xi}{U(y)} - \phi - t\right)\right] + O(\epsilon^3). \tag{5.3}$$

Unlike transient disturbances in an unbounded domain, the disturbance found here as a solution of the linearized equation is not a solution of the corresponding nonlinear equation, hence the presence of the $O(\epsilon^3)$ terms on the right-hand sides. The order of magnitude of these terms is obtained from (5.1) assuming that $b(0) = b(1) = 0$. In principle, the exact form of the nonlinear solution can be constructed using a regular perturbation expansion.

Significant instability is to be expected only when the vorticity gradient associated with (5.2) is of order one, i.e. when $\xi = O(\epsilon^{-1}\Omega^{-1})$. We make this assumption and note that a general stability study of the basic state given by (5.2)–(5.3) is difficult because of the basic-state dependence on ξ and t. To circumvent this difficulty, we follow Haynes (1987) in considering a particular case for which there is a scale separation between the basic state and the growing perturbations associated with the instability. Here, this particular case corresponds to the low-frequency limit $\Omega \ll 1$. Assuming this condition, we introduce the slow variables $\tilde{\xi} := \Omega\epsilon\xi$ and $\tilde{t} := \Omega(t + \phi)$ and rewrite the vorticity and streamfunction (5.2)–(5.3) as

$$\omega(\tilde{\xi}, y, \tilde{t}) = \frac{b(y)}{U(y)} \cos\left[\frac{\epsilon^{-1}\tilde{\xi}}{U(y)} - \tilde{t}\right] + O(\epsilon^3), \tag{5.4}$$

$$\psi(\tilde{\xi}, y, \tilde{t}) = -\epsilon^2 \frac{b(y)\,[U(y)]^3}{\lambda^2 \tilde{\xi}^2} \cos\left[\frac{\epsilon^{-1}\tilde{\xi}}{U(y)} - \tilde{t}\right] + O(\epsilon^3). \tag{5.5}$$

We consider a small-amplitude perturbation with vorticity $\tilde{\epsilon}\tilde{\omega}$ and streamfunction $\tilde{\epsilon}\tilde{\psi}$ (with $\tilde{\epsilon} \ll \epsilon$) superposed on $\epsilon\omega$ and $\epsilon\psi$ given by (5.4)–(5.5). This perturbation satisfies a linearized equation whose coefficients depend slowly on space and time through $\tilde{\xi}$ and $\tilde{t}$. However, it turns out that the fastest growing perturbations have

order-one scales in x (or, equivalently, ξ) and t; therefore we can employ a multiple-scale approach and seek normal-mode solutions of the form

$$\tilde{\omega} = \mathrm{Re}\left[\left(\frac{\mathrm{d}^2}{\mathrm{d}y^2} - k^2\right)\varphi(\tilde{\xi}, y, \tilde{t})\,\mathrm{e}^{\mathrm{i}k(\xi - ct)}\right], \quad \tilde{\psi} = \mathrm{Re}\left[\varphi(\tilde{\xi}, y, \tilde{t})\,\mathrm{e}^{\mathrm{i}k(\xi - ct)}\right],$$

regarding $\tilde{\xi}$ and $\tilde{t}$ as independent of ξ and t. The structure $\varphi(\tilde{\xi}, y, \tilde{t})$ is found to satisfy

$$(U - c)\left(\frac{\mathrm{d}^2\varphi}{\mathrm{d}y^2} - k^2\varphi\right) + \rho(\tilde{\xi}, y)\sin\left[\frac{\epsilon^{-1}\tilde{\xi}}{U(y)} - \tilde{t}\right]\varphi = O(\epsilon^2, \Omega), \tag{5.6}$$

$$\text{with} \quad \varphi(\tilde{\xi}, 0, \tilde{t}) = \varphi(\tilde{\xi}, 1, \tilde{t}) = 0,$$

where $\rho(\tilde{\xi}, y) := \lambda\tilde{\xi}b(y)/[U(y)]^3 = O(1)$. The terms of $O(\epsilon^2, \Omega)$ on the right-hand side of (5.6) govern the slow modulations of $\varphi(\tilde{\xi}, y, \tilde{t})$. These modulations have a secondary importance here, since we are mainly concerned with the instability mechanism. For simplicity, we then take $\Omega = O(\epsilon^2)$ or smaller: this choice ensures that to the order considered below the terms on the right-hand side of (5.6) can be ignored; it also implies that $\tilde{\xi}$ and $\tilde{t}$ can effectively be regarded as fixed parameters. To avoid cumbersome notation, in what follows we omit the (parametric) dependence of φ on $\tilde{\xi}$ and $\tilde{t}$ and we simply write $\varphi = \varphi(y)$.

Owing to the rapid variation in y of the sine function in (5.6), this equation can be solved using a multiple-scale method in the y-direction: the two variables y and $\eta := \epsilon^{-1}/U(y)$ are introduced, and φ and c are expanded in powers of ϵ according to

$$\varphi = \varphi^{(0)}(y, \eta) + \epsilon\varphi^{(1)}(y, \eta) + \cdots, \qquad c = c^{(0)} + \epsilon c^{(1)} + \cdots .$$

Substituting these expansions in (5.6) and replacing $\partial/\partial y$ by $-\epsilon^{-1}\lambda/U^2\partial/\partial\eta + \partial/\partial y$ we find at $O(\epsilon^{-2})$

$$\frac{\lambda^2(U - c^{(0)})}{U^4}\frac{\partial^2\varphi^{(0)}}{\partial\eta^2} = 0,$$

from which we conclude that $\varphi^{(0)}$ is a function of y only when $U - c^{(0)} = O(1)$. Similarly, the $O(\epsilon^{-1})$ equation indicates that $\varphi^{(1)}$ depends only on y. At $O(1)$, we find a non-homogeneous equation for $\varphi^{(2)}$ containing terms that are independent of η; solvability is ensured by imposing the vanishing of these terms, leading to

$$(U - c^{(0)})\left(\frac{\mathrm{d}^2\varphi^{(0)}}{\mathrm{d}y^2} - k^2\varphi^{(0)}\right) = 0, \quad \text{with} \quad \varphi^{(0)}(0) = \varphi^{(0)}(1) = 0. \tag{5.7}$$

A non-trivial solution exists only if $U(0) < c^{(0)} < U(1)$; it is given by the Green's function (2.7) according to

$$\varphi^{(0)} = A\,G(y, y^{(0)}, k), \tag{5.8}$$

where $y^{(0)}$ is defined by $U(y^{(0)}) = c^{(0)}$ and A is an arbitrary constant.

The Green's function is not smooth for $y \approx y^{(0)}$, so that (5.7) is not valid for $y - y^{(0)} = O(\epsilon)$. In this (inner) region, φ varies rapidly in y, and a new expansion needs to be employed. (Note that $y^{(0)}$ is essentially a free parameter that can be interpreted physically as the location at which a perturbation vorticity $\tilde{\omega}$ is introduced, since $\tilde{\omega}$ is non-zero at leading order in the inner region only.) The inner expansion may be written

$$\varphi = \Phi^{(0)}(Y) + \epsilon\Phi^{(1)}(Y) + \cdots,$$

where the stretched coordinate Y, defined by $y = y^{(0)} + \epsilon Y$, is used instead of η.

Introducing this expansion in (5.7) and matching with (5.8) leads to the leading-order solution

$$\Phi^{(0)} = A\, G(y^{(0)}, y^{(0)}, k). \tag{5.9}$$

At next order one finds the equation

$$(\lambda Y - c^{(1)})\frac{\mathrm{d}^2\Phi^{(1)}}{\mathrm{d}Y^2} + \rho(\tilde{\xi}, y^{(0)}) \sin\left[\delta - \frac{\lambda\tilde{\xi}}{(c^{(0)})^2} Y\right] \Phi^{(0)} = 0, \tag{5.10}$$

where $\delta := (\epsilon^{-1}\tilde{\xi}/c^{(0)} - \tilde{t}) \bmod 2\pi$ is a fixed parameter. The matching condition for $\Phi^{(1)}$ is

$$\int_{-\infty}^{\infty} \frac{\mathrm{d}^2\Phi^{(1)}}{\mathrm{d}Y^2}\,\mathrm{d}Y = \left[\frac{\mathrm{d}\varphi^{(0)}}{\mathrm{d}y}\right]_{y_-^{(0)}}^{y_+^{(0)}} = A,$$

where the second equality stems from (5.8) and from the definition of the Green's function. Taking (5.9)–(5.10) into account, this condition leads to the dispersion relation in the implicit form

$$\int_{-\infty}^{\infty} \frac{1}{\lambda Y - c^{(1)}} \sin\left[\delta - \frac{\lambda\tilde{\xi}}{(c^{(0)})^2} Y\right] \mathrm{d}Y = \frac{-1}{\rho(\tilde{\xi}, y^{(0)})\, G(y^{(0)}, y^{(0)}, k)}.$$

This integral can be evaluated using the residue theorem; after some manipulations, the imaginary part of $c^{(1)}$ is written as

$$\begin{aligned} \operatorname{Im} c^{(1)} &= -\frac{(c^{(0)})^2}{\tilde{\xi}} \log\left|\frac{\lambda}{\rho(\tilde{\xi}, y^{(0)})\, G(y^{(0)}, y^{(0)}, k)}\right| \\ &= -\frac{(c^{(0)})^2}{\tilde{\xi}} \log\left\{\frac{(c^{(0)})^3 k}{\tilde{\xi} b(y^{(0)})}\left[\coth(k y^{(0)}) + \coth[k(1 - y^{(0)})]\right]\right\} \end{aligned} \tag{5.11}$$

when it is positive, corresponding to an instability. The sheared disturbance is therefore unstable when the argument of the logarithm is smaller than 1. Since the function of k present in the argument is minimum for $k \to 0$ and then equals $[y^{(0)}(1 - y^{(0)})]^{-1}$ we conclude that there is an instability provided that

$$\frac{(c^{(0)})^3}{\tilde{\xi} b(y^{(0)}) y^{(0)}(1 - y^{(0)})} < 1.$$

A few remarks can be made. First, the flow is always unstable when $\tilde{\xi}$ is sufficiently large, i.e. at a sufficient distance downstream of the source. However, it is not unconditionally unstable at fixed $\tilde{\xi}$, although there is a reversal of the vorticity gradient regardless of $\tilde{\xi}$. The reason for this is the stabilizing effect of the boundaries (absent in Haynes' 1987 study); this is clear when one notes that, in an unbounded domain, the coth functions in (5.11) are replaced by 1, so the system is systematically unstable for small enough k. Another clear effect of the boundaries is the fact that perturbations with leading-order phase velocities close to the basic velocity at the boundaries (i.e. with $y^{(0)} \approx 0$ or $y^{(0)} \approx 1$) are stable. The centre of the channel thus appears as the most unstable region of the flow, provided that $b(\frac{1}{2}) \neq 0$. Finally, we note that the instability with $k \ll 1$ should be taken with caution because, in this limit, there is no clear scale separation between the streamwise variations of the basic state (the sheared disturbance) and those of the infinitesimal perturbation. Nevertheless, as figure 7 illustrates, the maximum growth rate of the instability is generally attained for $k = O(1)$ in which case the scale-separation assumption is strictly valid.

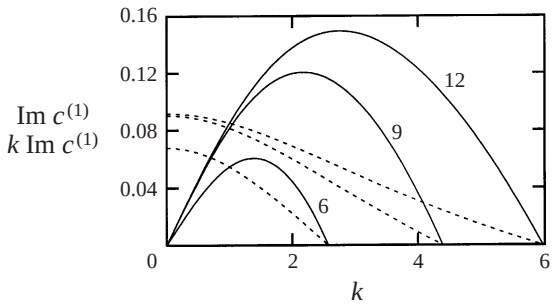

FIGURE 7. Growth rate $k\,\mathrm{Im}\,c^{(1)}$ (solid lines) and $\mathrm{Im}\,c^{(1)}$ (dashed lines) against wavenumber k, as obtained from (5.11) with $b(y^{(0)})/c^{(0)} = 1$ and $\tilde{\xi}/(c^{(0)})^2 = 6, 9, 12$.

Figure 7 shows the growth rate $k\,\mathrm{Im}\,c^{(1)}$ and $\mathrm{Im}\,c^{(1)}$ as functions of the wavenumber k, assuming $y^{(0)} = \frac{1}{2}$ and $b(y^{(0)})/c^{(0)} = 1$; the only parameter left, $\tilde{\xi}/(c^{(0)})^2$, is taken equal to 6, 9 and 12 (its minimum value for instability is 4). For comparison with Haynes' (1987) results, it can be noted that the fastest-growing instability is obtained for $\tilde{\xi}/(c^{(0)})^2 \to \infty$ with $k = \tilde{\xi}/[2\,\mathrm{e}(c^{(0)})^2]$ and corresponds to a growth rate $k\,\mathrm{Im}\,c^{(1)} = 1/(2\,\mathrm{e}) = 0.1839$.

6. Conclusion

In this note, we have studied the linear response of a two-dimensional Couette flow to a time-periodic forcing. The forcing, represented by a vorticity source, is distributed along a straight line of arbitrary orientation. This problem can be regarded as the spatial analogue of the initial-value problem in which one studies the response of the flow to a spatially periodic initial excitation. For this initial-value problem, initial conditions corresponding to constant-vorticity lines tilted against the shear lead to a transient growth of the disturbance energy which is not captured by spectral stability analysis. Here, in an analogous manner, a spatially localized growth of the energy – not captured by the signalling problem – is shown to occur when the vorticity source is tilted against the shear. The energy maximum may be located far downstream of the source; it is notably so when the vorticity source is strongly tilted. The long-distance behaviour of the disturbance streamfunction and energy (shown to decay like x^{-2}), the self-consistency of the linearization, and the disturbance instability are examined, leading to results which parallel those obtained for the initial-value problem.

Although we have restricted our investigation to Couette flows, it is clear that the analysis reported in this note can be extended to flows with non-zero cross-stream vorticity gradient, i.e. to flows with curved velocity profiles and/or with β-effect. As is the case for transient disturbances, one may expect the conclusions obtained here to carry over to these more complex flows in so far as their velocity profiles are monotonic. For non-monotonic profiles, however, the behaviour of the disturbance may certainly be very different; following the analysis of the initial-value problem by Brunet & Warn (1990) and Brunet & Haynes (1995), we anticipate the linearization not to be self-consistent if the cross-stream vorticity gradient is weak. The spatial, as opposed to temporal, development of a nonlinear critical layer that probably appears in this situation deserves a detailed examination.

A key assumption of our analysis is that of a strictly two-dimensional flow. This limits its relevance for plane Couette flows in which two-dimensionality is not imposed externally (as can be done e.g. through strong rotation): for such flows, which

have been extensively studied both experimentally (e.g. Dauchot & Daviaud 1995) and numerically (e.g. Komminaho, Lundbladh & Johanson 1996), three-dimensional effects play a major role, leading, for instance, to algebraic disturbance amplification, both spatially and temporally (e.g. Luchini 1996 and references therein).

It is a pleasure to acknowledge helpful conversations with T. Warn.

REFERENCES

Briggs, R. J. 1964 *Electron-Stream Interactions in Plasmas*. MIT Press.

Brown, S. & Stewartson, K. 1980 On the algebraic decay of disturbances in stratified shear flows. *J. Fluid Mech.* **100**, 811–816.

Brunet, G. & Haynes, P. H. 1995 The nonlinear evolution of disturbances to a parabolic jet. *J. Atmos. Sci.* **52**, 464–477.

Brunet, G. & Warn, T. 1990 Rossby wave critical layers on a jet. *J. Atmos. Sci.* **47**, 1173–1178.

Dauchot, O. & Daviaud, F. 1995 Streamwise vortices in plane Couette flow. *Phys. Fluids* **7**, 901–903.

Farrell, B. F. 1990 Small error dynamics and the predictability of atmospheric flows. *J. Atmos. Sci.* **47**, 2409–2416.

Farrell, B. F. & Ioannou, P. J. 1993 Stochastic forcing of the linearized Navier–Stokes equations. *Phys. Fluids* A **5**, 2600–2609.

Farrell, B. F. & Ioannou, P. J. 1996 Generalized stability theory. Part I: autonomous operators. *J. Atmos. Sci.* **53**, 2025–2040.

Haynes, P. H. 1987 On the instability of sheared disturbances. *J. Fluid Mech.* **175**, 463–478.

Henningson, D. S., Gustavsson, L. H. & Breuer, K. S. 1994 Localized disturbances in parallel shear flows. *Appl. Sci. Res.* **53**, 51–97.

Huerre, P. & Monkewitz, P. A. 1985 Absolute and convective instabilities in shear layers. *J. Fluid Mech.* **159**, 151–168.

Huerre, P. & Monkewitz, P. A. 1990 Local and global instabilities in spatially developing flows. *Ann. Rev. Fluid Mech.* **22**, 473–537.

Ichimaru, S. 1973 *Basic Principles of Plasma Physics: A Statistical Approach*. W. A. Benjamin.

Kominaho, J., Lunbladh, A. & Johansson, A. V. 1996 Very large structures in plane turbulent Couette flow. *J. Fluid Mech.* **320**, 259–285.

Luchini, P. 1996 Reynolds-number-independent instability of the boundary layer over a flat surface. *J. Fluid Mech.* **327**, 101–115.

Orr, W. M. F. 1907 The stability and instability of the steady motion of a perfect liquid and a viscous liquid. Parts I and II. *Proc. R. Irish Acad.* A **27**, 9–138.

Shepherd, T. G. 1985 Time development of small disturbances to plane Couette flow. *J. Atmos. Sci.* **42**, 1868–1871.

Thomson, W. 1887 Stability of fluid motion – rectilineal motion of viscous fluid between two parallel planes. *Phil. Mag.* **24**, 188–196.

Trefethen, L. N., Trefethen, A. E., Reddy, S. C. & Driscoll, T. B. 1993 Hydrodynamics stability without eigenvalues. *Sciences* **261**, 578–584.

Tung, K. K. 1983 Initial-value problem for Rossby waves in a shear flow with critical level. *J. Fluid Mech.* **133**, 443–469.